# Evaluation of X-ray Induced Degradation of Light Response and Dark Current in BSI CMOS Image Sensors with Backside Deep Trench Isolation

Toshiyuki Isozaki, Ken Miyauchi, Rimon Ikeno, and Junichi Nakamura, Brillnics Japan Inc., Tokyo, Japan
Contact: Toshiyuki Isozaki: phone: +81-3-6404-8801, fax: +81-3-5767-5568,
email: isozaki.toshiyuki@brillnics.com

## 1. Introduction

Radiation degradation of image sensors is well investigated for medical and space applications with X-ray dose ranging from a few kGy to GGy. Even with image sensors for consumer applications, reliability or robustness against X-ray degradation is required to endure shipping tests. This paper reports X-ray degradation that was observed with a prototype 4.6 µm backside illuminated (BSI) digital pixel sensor (DPS) fabricated in a 45nm / 65nm stacked process (Chip A) [1] after 0.1Gy to 50 Gy X-ray irradiation. While the issue of X-ray degradation has been solved in the latest fabrication lots, the findings through this investigation should be worth sharing with the imaging community. Especially, it is suggested that dark signal increase comes from interface states of the shallow-trench isolation (STI), dark signal increase and light responsivity degradation come from those of the pyramid surface for diffraction (PSD) structure for near infrared (NIR) sensitivity enhancement and backside deep-trench isolation (BDTI) structure.

## 2. Experiments

### 2.1 Experiment overview

We studied X-Ray radiation impact on a stacked digital pixel sensor (Chip A)[1] whose pixel schematics are presented in Fig. 1. Other 5 sensors (Table 1 : Chip B, C, D, E, and F) were also analyzed together as the references to study the fabrication technology dependence. X-ray from 0.1Gy to 50 Gy (air Kerma) was irradiated to the sensors at room temperature with a dose rate of 1Gy/min and the average energy of ~40 keV. The samples wer not powered during the irradiation.

### 2.2 Pixel performance impact by X-ray irradiation

Typical images and thier signal-level distributions after X-ray irradiation are shown in Fig. 2. The images were captured using Chip A after 10Gy irradiation. Figs. 2 (a) and (c) are for the image captured with 700-ms integration time under the dark condition at room temperature. Figs. 2 (b) and (d) are for the images captured under an illuminated condition with 1-ms integration time (Tint) at room temperature (RT). The dark image shows a high-side peak and the distribution tail with higher signal levels. They are considered to be due to increase of dark current by the irradiation. The middle-light image shows a low-side peak by the pixels with the lower responsivity.

### 2.3 Responsivity degradation

Prior studies using front-side illumination (FSI) sensors [2, 3] reported that increase of surface recombination velocity by increase of interface state density by X-ray radiation causes the degradation of quantum efficiency. Fig. 3 shows the light wavelength dependence of signal level distribution. Intensity of each color LED was adjusted to obtain identical mid-level outputs of normal pixels. Shorter wavelength light causes a larger decrease in output levels of responsivity degraded pixels. This result indicates that the origin of the responsivity degradation is located near the backside surface.

### 2.4 Correlation between light responsivity and dark current degradation

Fig. 4 shows pixel-wise scattering plots of the signal levels at middle-light condition (Tint = 65ms, RT) and those at dark (Tint = 700ms, RT). The X-ray irradiation was varied from 0 Gy to 50 Gy. 3 types of pixels were found; 1) pixels with no-degradation, 2) pixels with dark-level increase (Type A), and 3) pixels with dark-signal increase and light-responsiviry decrease (Type B). To narrow down the damaged regions causing Type-A and Type-B degradations, the dark current generated in FD was evaluated by comparing the images with and without signal-charge transfer from PD. Fig. 5 shows the pixel-wise correlation of the responsivity represented by the middle-light signal with charge transfer from PD in Y axis and the dark current generated in FD without charge transfer from PD in X axis. Type-A pixels in the black circle still show the dark-signal increase without charge transfer. Then, we can say that the origin of Type-A pixel's dark current is not in PD. Fig. 5 also suggests that the damaged part of Type-B pixels (in red dotted circle) is estimated to be inside PD because they did not show performance variation if signal charges in PD are not transferred. Furthemore, we can say that damaged part of Type-B is near the backside in the PD according to the discussion in section 2.3.

### 2.5 X-ray induced responsivity degradation in other sensors

To obtain further information on possible locations of the origin of the X-ray induced responsivity degradation, other 5 types of sensors (Table 1) were analyzed. Layouts and cross-sectional views of the pixels of these chips are depicted in Table 2. They have variations in stacked/non-stack, PSD, and BDTI structures.

Fig. 6 and 7 show signal level distributions of the stacked BSI sensors (Chips B and C) and the non-stacked BSI sensors (Chips D, E, and F) with 1ms integration time at room temperature with 50Gy dose. Comparing the distributions of Chip B and C, Chip B had the tail in the lower side but Chip C did not. Chip B and C is different in the presence of the PSD structure, while BDTI is formed in the both chips. The signal distribution of Chip D is slightly worse than that of Chip E, possibly due to BDTI structure that is formed in Chip D but not in Chip E. Then, it is likely that an origin of the X-ray induced degradation is located around BDTI. Though Chip F has a larger pixel than Chip E, it has similar structure in PSD and BDTI, and showed no degradation like Chip E. These results imply that the responsivity degradation comes from interface states at PSD, or interface states at BDTI that originate from the PSD structure.

## 3. Summary

X-ray induced degradations of light response and dark current have been investigated using a prototype DPS. Two types of degraded pixels were observed. One is with degradation in dark current and the other is with degradation in responsivity and dark current. Evaluation results suggest that the former degradation comes from interface states around the STI, and the latter degradation comes from those around the PSD and BDTI. This implication is consistent with evaluation results of other sensors with different pixel structures. Also, irradiating X-rays can be a way to identify a weak point in a CIS pixel and/or in process steps.

## References

[1] R. Ikeno et al., “A 4.6-μm, 127-dB dynamic range, ultra-low power stacked digital pixel sensor with overlapped triple Quantization,” IEEE Trans Electron Devices, vol. 69, no. 6, pp. 2943-2950, JUNE 2022

[2] Jiaming Tan et al., “Analyzing the radiation degradation of 4-transistor deep submicron technology CMOS image sensors,” Sensors, vol. 12, no. 6, pp. 2278-2286, JUNE 2012

[3] V. Goiffon et al., “Overview of ionizing radiation effects in image sensors fabricated in a deep-submicrometer CMOS imaging technology,” IEEE Trans. Electron Devices, vol. 56, no. 11, pp. 2594-2601, Nov. 2009

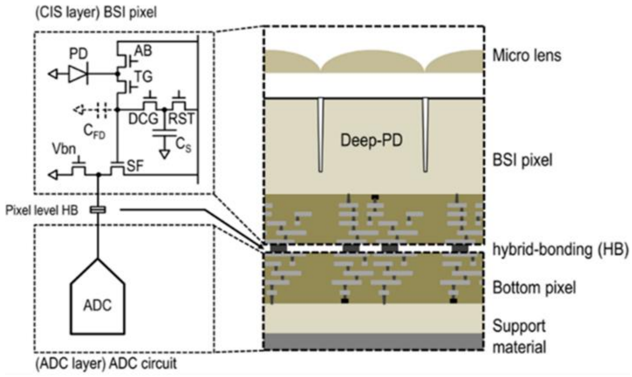


Fig. 1: Circuit diagram and cross-sectional view of the stacked DPS in [1]

Table 1: Studied chip information

| Chip | PSD | BDTI | Process | Pixel size |
|---|---|---|---|---|
| Chip A | Yes | Yes | 45nm BSI / 65nm stack | 4.6 µm |
| Chip B | Yes | Yes | 45nm BSI / 40nm stack | 1.98 µm |
| Chip C | No | Yes | 45nm BSI / 40nm stack | 1.98 µm |
| Chip D | Yes | Yes | 65nm BSI | 2.12 µm |
| Chip E | No | No | 65nm BSI | 2.12 µm |
| Chip F | No | No | 65nm BSI | 3.0 µm |

Table 2: Layout and cross section of the analyzed image-sensor pixels

| Stack | Layout / Cross section | | |
|---|---|---|---|
| 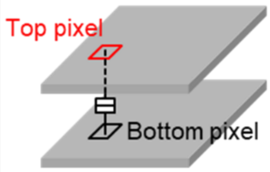  | Chip A 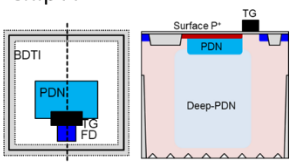  | Chip B 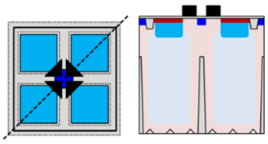 | Chip C 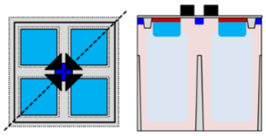 |
|   | Chip D 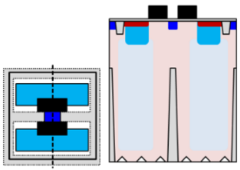 | Chip E 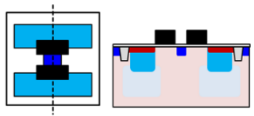 | Chip F 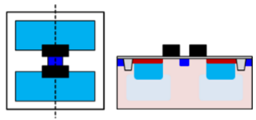 |

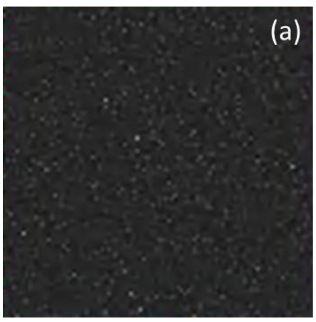


(a) Dark image (Tint = 700 ms)

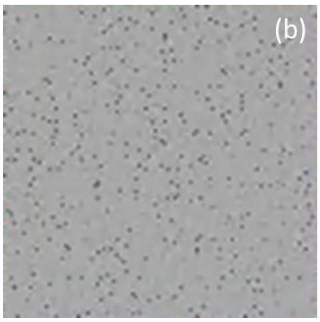


(b) Middle-light image (Tint = 65 ms)

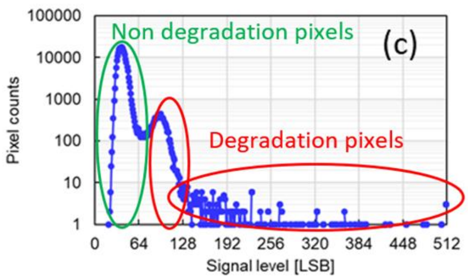


(c) Signal distribution of the original image of (a)

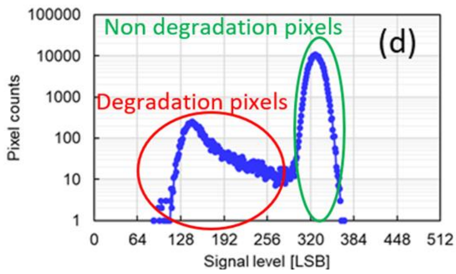


(d) Signal distribution of the original image of (b)

Fig. 2: Images and signal distributions of ChipA with 10 Gy dose at room temperature

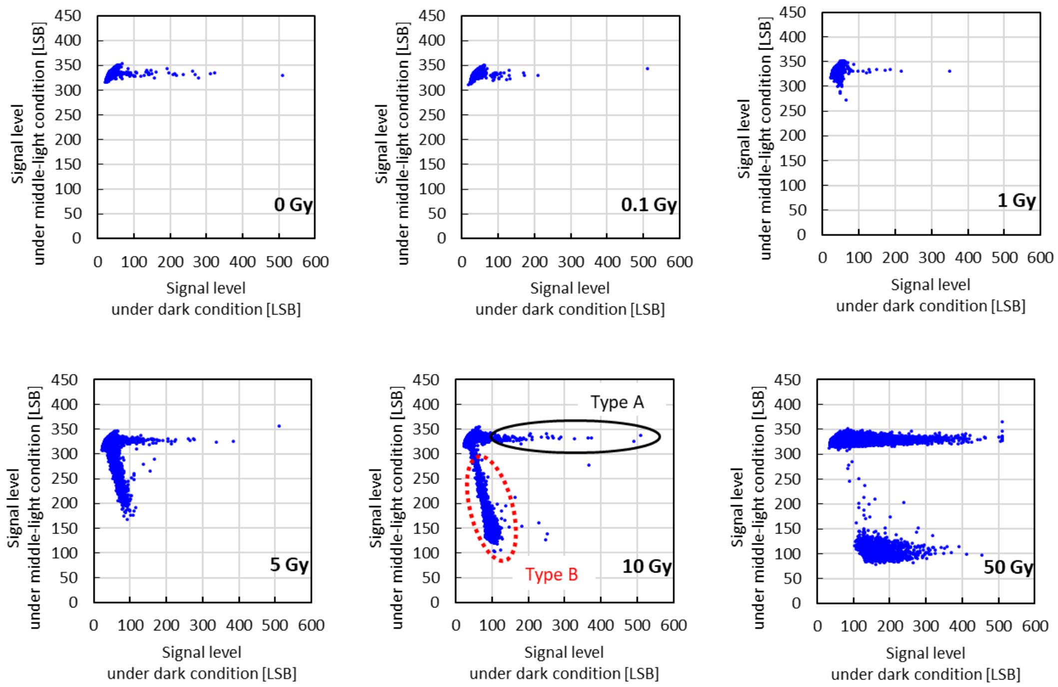


Fig.4: Pixel-wise correlation of signal levels under middle-light (Tint = 65ms) and dark condition (Tint = 700ms)

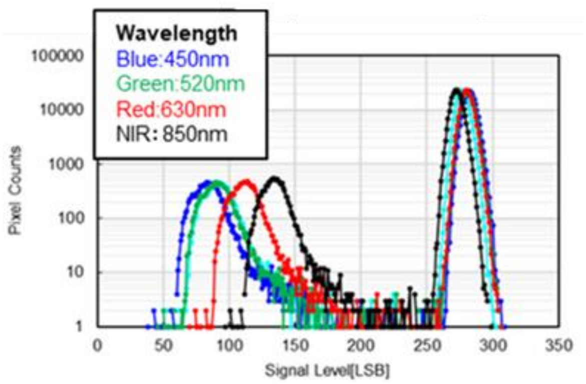


Fig. 3: Wavelength dependence of signal level distribution

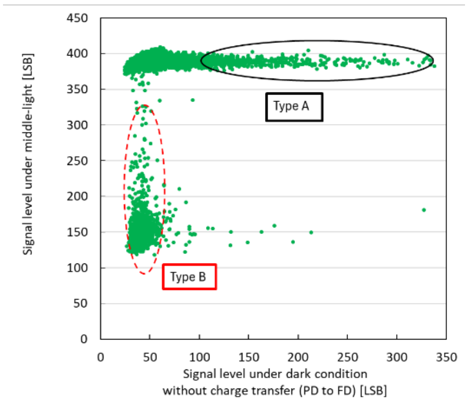


Fig. 5: Pixel-wise correlation of signal levels under middle-light condition (Tint =1 ms) and under dark condition without PD charge transfer (Tint = 700 ms)

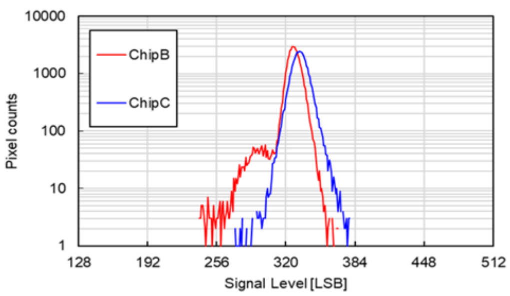


Fig. 6: Signal distribution of Chip B and C under middle-light condition with 10Gy dose (Tint = 1 ms)

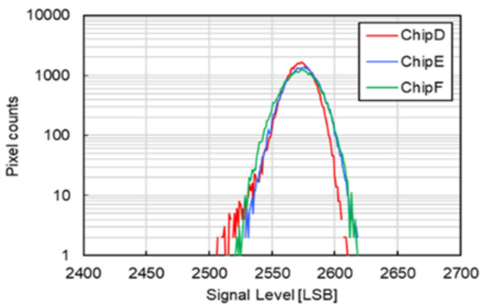


Fig. 7: Signal distribution of Chip D, E and F under middle-light condition with 10Gy dose (Tint = 1 ms)